

Bloch oscillations of atoms in an optical multiphoton potential

Tobias Salger,¹ Gunnar Ritt,^{2,*} Carsten Geckeler,^{1,2} Sebastian Kling,¹ and Martin Weitz¹

¹*Institut für Angewandte Physik, Universität Bonn, Wegelerstr. 8, D-53115 Bonn*

²*Physikalisches Institut, Universität Tübingen,*

Auf der Morgenstelle 14, D-72076 Tübingen

(Dated: November 14, 2007)

Abstract

We report on experiments studying transport properties of an atomic Bose-Einstein condensate in an optical lattice of spatial period $\lambda/2n$, where n is an integer, realized with the dispersion of multiphoton Raman transitions. We observe Bloch oscillations, as a clear effect of quantum transport, in the sub-wavelength scale periodicity lattice. The unusually strong localisation of atoms is evident from the measured effective mass. Future prospects of the novel lattice structures are expected in the search for new quantum phases in tailored lattice structures up to quantum computing in optical nanopotentials.

PACS numbers: 03.75.Lm, 32.80.Pj, 42.50.Vk

*Present address: FGAN-FOM, Gutleuthausstraße 1, D-76275 Ettlingen

Considering their spatial periodicity of $\lambda/2$ from trapping site to trapping site, conventional optical lattices, formed by atoms confined in the antinodes of optical standing waves by light forces, just operate at the Rayleigh resolution limit [1]. Motivated by the quest to write smaller lithographic features, multiphoton and entangled photon techniques have been investigated for the creation of smaller sized spatial structures [2–4]. In general, a n -photon process can lead to a n -fold increase in the spatial resolution.

In our experiment we study Bloch oscillations of atoms in lattices for which the lattice periodicity is clearly below the Rayleigh resolution limit. The smaller spatial periodicity of the investigated tightly bound multiphoton lattices leads to a larger Bloch period. Within our experimental uncertainties, no Bragg diffraction signal is observed when accelerating atoms in the multiphoton lattice to the first band edge of the conventional lattice. The transport signals along with the determined effective mass in a $\lambda/4$ -periodicity multiphoton lattice are compared to the results obtained with a conventional lattice of $\lambda/2$ spatial periodicity.

Optical lattices have developed into successful model systems for effects known or predicted in solid state physics [5]. Bloch oscillations, in which an atom subject to a force performs an oscillatory rather than a uniformly accelerated motion, are one of the most striking quantum transport property arising from the periodic potential [6]. In other works, concepts as number squeezing [7] or the Mott-insulator transition [8] were investigated. Further, Landau-Zener transitions have been studied in optical lattices of variable spatial symmetry [9].

Let us begin by describing our scheme to create sub-Rayleigh resolution optical lattices for cold atoms. The trapping potential of conventional lattices is determined by the ac Stark shift in optical standing waves. In a quantum picture, the absorption of one photon of a running wave mode followed by the stimulated emission of a photon into a counterpropagating mode contribute to the trapping potential. A lattice with spatial periodicity of a fractional harmonic $\lambda_{\text{eff},n}/2 = \lambda/2n$ could in principle be achieved by replacing each of the absorption and emission cycles with a stimulated multiphoton process induced by n photons, as indicated in Fig. 1a. Here, $\lambda_{\text{eff},n}$ denotes the effective wavelength of a n -photon field [10]. Fig. 1b shows the used scheme for a four- and six-photon lattice with potential periodicities of $\lambda/4$ and $\lambda/6$ correspondingly [9, 11–13]. In this improved scheme, absorption (stimulated emission) processes have been exchanged by stimulated emission (absorption) processes of an oppositely directed photon. The high resolution of Raman spectroscopy between two

stable ground states over an excited state here allows to clearly separate in frequency space the desired $2n$ -order process from lower order contributions. Our experimental setup has been described previously [11, 14]. Briefly, a rubidium (^{87}Rb) Bose-Einstein condensate is produced all-optically by evaporative cooling in a quasistatic CO_2 -laser dipole trap. During the final stages of the evaporation, a magnetic field gradient is activated, resulting in a spin-polarized condensate with roughly 10^4 atoms in the $m_F = -1$ Zeeman component of the $F = 1$ hyperfine ground state. The lattice beams are generated by splitting the emitted beam of a tapered diode laser into two and directing each of the partial beams through an acoustooptic modulator. The modulators are used for beam switching, and also to superimpose different optical frequency components onto a single beam path, as required for generation of the multiphoton potentials with the schemes shown in Fig. 1b. The beams are sent through optical fibres and focused in a counterpropagating geometry onto the Bose-Einstein condensate. Respectively to the horizontally oriented CO_2 -laser dipole trapping beam, the lattice beams are inclined under an angle of 41° degrees. For the realization of multiphoton lattices shown in Fig. 1b, we use the $F = 1$ ground state Zeeman components $m_F = -1$ and 0 as levels $|g_0\rangle$ and $|g_1\rangle$, and the $5\text{P}_{3/2}$ manifold as the excited state $|e\rangle$. A magnetic bias field of 1.8 G removes the degeneracy of the Zeeman components. For a measurement of Bloch oscillations, the lattice beams are initially ramped up with a linear ramp within $20 \mu\text{s}$ to adiabatically load the atoms into the lowest band of the lattice potential. This procedure was applied for the usual two-photon as well as for the multiphoton lattice potentials. One of the lattice beams was subsequently acoustooptically detuned with a constant chirp rate (for the four-photon lattice scheme on the left hand side of Fig. 1b, the single beam with frequency ω was used) to accelerate the lattice respectively to the atomic rest frame. After a variable acceleration time, the lattice beams were extinguished and the atomic momentum distribution was recorded with a time-of-flight absorption imaging technique. In initial experiments, we have studied far field diffraction of atoms off the lattice potentials. The atoms here were exposed to the periodic potentials imprinted by $6 \mu\text{s}$ long optical pulses of the lattice beams. Fig. 2 shows corresponding atomic time-of-flight images recorded after a 12 ms long free expansion time and reconstructed lattice potentials for (a) a conventional lattice, (b) a four-photon lattice and (c) a six-photon lattice. For the higher order multiphoton lattices, the spacing between diffraction orders is increased due to the smaller spacing between sites of the corresponding periodic potential. For sufficiently short

pulses and small pulse areas the time-of-flight images are closely connected to the reciprocal lattice, but also for more general pulses an analysis of such images allows for a determination of lattice parameters [10].

Quantum transport of cold atoms in optical lattices much resembles the behaviour of electrons in crystal lattices [15]. In a one-dimensional atom potential of the form $V(x) = V_0 \cos^2(\pi x/d)$, where $d = \lambda/2n$ denotes the lattice periodicity with n as an integer number and V_0 the lattice depth, the energy spectrum splits up into bands. They can be labelled by the Eigenenergies $E_j(q)$ of the Eigenstates $|j, q\rangle$, where j denotes the band index and q the atomic quasimomentum, and $E_j(q)$ and $|j, q\rangle$ are periodic functions of the quasimomentum q with period $2\pi/d = 4\pi \cdot n/\lambda$. Conventionally, the quasimomentum q is restricted to the first Brillouin zone, i. e.: $|q| \leq \hbar\pi/d = n \cdot \hbar k$. Thus, the first Brillouin zone of a $2n$ -th order multiphoton lattice with spatial periodicity $\lambda/2n$ spans a n -fold larger quasimomentum range than a conventional standing wave lattice of periodicity $\lambda/2$. At the first band gap, states with quasimomentum $q \in \{-n\hbar k, n\hbar k\}$ are coupled due to Bragg reflection, which leads to an energy splitting between the lowest and the first excited band, and similar couplings also occur between higher bands. When an external force F is applied which is weak enough not to cause Landau-Zener transitions to other bands, the quasimomentum evolves in time according to $q(t) = q(0) + F \cdot t$. At the band gaps we expect that the wavepackets are Bragg-reflected, so that the evolution is periodic in time, and $T_B = n \cdot \hbar k/F$ denotes the period, required for the wavepacket to evolve over the full Brillouin zone. The atomic group velocity $\langle v \rangle = dE(q(t))/dq$ here oscillates with time. The expected band structure for our lattice potentials is shown in Fig. 3 for a two- and four-photon lattice respectively. Experimentally we have adjusted the depth of the lattice potentials for both lattices to be around $2.7 E_r$ (with $E_r = \hbar^2 k^2/2m$ corresponding to the photon recoil energy), as was monitored by Rabi oscillations [16]. For a measurement of Bloch oscillations, the atomic Bose-Einstein condensate is adiabatically loaded into the lowest band of the lattice potentials at zero quasimomentum ($q = 0$). Subsequently, the lattice potential is accelerated respectively to the atomic rest frame by applying a linear variation of one of the Raman beams frequency. In this way, a constant inertial force $F = -ma$ is exerted onto the atoms. Fig. 4 shows the mean atomic velocity relatively to the lattice as a function of acceleration time t_a for both two- and four-photon lattice potentials. For small acceleration times, the atomic velocity increases linearly with time, as predicted by Newtons second law for a free atom. We expect

that an acceleration continues until the edge of the first Brillouin zone, which is reached at a quasimomentum $q = \hbar\pi/d$, where $d = \lambda/2n$ denotes the spacing from site to site. With $n = 1$ and 2 for two- and four-photon lattices, the band edge occurs at $q = \hbar k$ and $2\hbar k$ respectively, as shown in Fig. 3. For the conventional two-photon lattice, we as in earlier work [6] observe, that the wavepacket is Bragg reflected near $F \cdot t_a \approx \hbar k$. On the other hand, for the $\lambda/4$ spatial periodicity four-photon lattice the atoms are accelerated until $F \cdot t_a \approx 2\hbar k$ is reached. In both cases Bragg reflection occurs at the corresponding band gap. The atomic wavepackets are reflected to the corresponding negative momentum value and full Bloch oscillations are observed. The demonstration of this phenomenon for a $\lambda/4$ periodicity multiphoton lattice directly shows the coherence of atom transport in such sub-Rayleigh periodicity structures. Notably, this study of quantum transport in high periodicity lattices significantly differs from earlier static atom optic diffraction experiments with high momentum transfer [17–19]. The Bloch-period T_B in the smaller periodicity four-photon lattice is a factor two longer than that of the conventional lattice. A more detailed comparison of the shapes of the observed oscillations in Fig. 4, both of which were recorded for comparable lattice depths, shows, that the slope steepness near the band edge is larger in the multiphoton lattice than that of the standing wave potential. Furthermore, the atomic acceleration near zero momentum is very similar to that of a free atom for the microscopic $\lambda/4$ periodicity lattice, while a somewhat larger difference is observed for the conventional lattice. These effects can be described in terms of the effective masses m^* . The atomic dynamics can be described using the usual equation of motion $F = m^*d\langle v \rangle/dt$ when accounting for an effective mass $m^*(q) = 2/(d^2E/dq^2)$, which in general differs from the free atomic mass due to the periodic potential. The dashed lines in Fig. 3 give the expected dependences of m^* on the atomic quasimomentum. For the smaller periodicity four-photon lattice, the effective mass near $q = 0$ is much closer to the real atomic mass than in the usual $\lambda/2$ periodicity lattice, which is easily understood in terms of the larger distance from the band-edge for the multiphoton lattice. This clearly shows the by a factor four stronger binding of this high periodicity lattice. Further, near the band edge the (negative) effective mass reaches smaller absolute values. This issue could be important in future studies of the Tonks-Girardeau regime in one-dimensional structures, where small effective masses are required [20]. Our transport measurements clearly reveal effects arising from the tight binding of the multiphoton lattice, as is evident when considering the quadratic scaling of the energy of the first band gap

$\epsilon_g(n) = (n\hbar k)^2/2m = n^2 E_r$ on the order $2n$ of the multiphoton lattice.

To conclude, we have observed Bloch-oscillations of atoms in a novel, sub-Rayleigh periodicity optical lattice. Evidence for a comparatively strong localization of atoms in the short periodicity lattice is obtained from the measured effective atomic mass. We expect that the observed effects can have applications in the development of nanoscale quantum computing schemes and the modelling of solid state physics problems. Note that a reaching of e.g. the Mott-insulator transition in short-periodicity lattices is favoured by larger tunnelling rates and stronger interatomic interactions with a decreased spacing from site to site. An alternative perspective includes the Fourier-synthesis of arbitrarily shaped lattice structures with quantum gases realized by superimposing lattices of different spatial periodicities, which allows for a dynamic tailoring of solid-state like structures.

We acknowledge financial support from the Deutsche Forschungsgemeinschaft and the Landesstiftung Baden-Württemberg.

-
- [1] See, e.g.: P.S. Jessen and I.H. Deutsch, *Adv. Atm. Mol. Opt. Phys.* **37**, 95 (1996).
 - [2] E. Yablonovitch and R.B. Vrijen, *Opt. Eng.* **38**, 334 (1999).
 - [3] A.N. Boto, P. Kok, D.S. Abrams, S.L. Braunstein, C.P. Williams, and J.P. Dowling, *Phys. Rev. Lett.* **85**, 2733 (2000).
 - [4] S. Bentley and R. Boyd, *Optics Express* **12**, 5735 (2004).
 - [5] See, e.g.: I. Bloch, *Nature Physics* **1**, 23 (2005).
 - [6] M. Ben Dahan, E. Peik, J. Reichel, Y. Castin, and C. Salomon, *Phys. Rev. Lett.* **76**, 4508 (1996).
 - [7] C. Orzel, A.K. Tuchman, M.L. Fenselau, M. Yasuda, and M.A. Kasevich, *Science* **291**, 2386 (2001).
 - [8] M. Greiner, O. Mandel, T. Esslinger, T.W. Hänsch, and I. Bloch, *Nature* **415**, 39 (2002).
 - [9] T. Salger, C. Geckeler, S. Kling, and M. Weitz, *Phys. Rev. Lett.* **99**, 190405 (2007).
 - [10] J. Jacobson, G. Bjork, I. Chuang, and Y. Yamamoto, *Phys. Rev. Lett.* **74**, 4835 (1995).
 - [11] G. Ritt, C. Geckeler, T. Salger, G. Cennini, and M. Weitz, *Phys. Rev. A* **74**, 63622 (2006).
 - [12] P.R. Berman, B. Dubetsky, and J.L. Cohen, *Phys. Rev. A* **58**, 4801 (1998).
 - [13] M. Weitz, G. Cennini, G. Ritt, and C. Geckeler, *Phys. Rev. A* **70**, 43414 (2004).

- [14] G. Cennini, G. Ritt, C. Geckeler, and M. Weitz, *Phys. Rev. Lett.* **91**, 240408 (2003).
- [15] N.W. Ashcroft and N.D. Mermin, (Saunders College Publishing, New York, 1976).
- [16] O. Morsch, J.H. Muller, M. Cristiani, D. Ciampini, and E. Arimondo, *Phys. Rev. Lett.* **87**, 140402 (2001).
- [17] P.E. Moskowitz, P.L. Gould, S.R. Atlas, and D.E. Pritchard, *Phys. Rev. Lett.* **51**, 370 (1983).
- [18] D.M. Giltner, R.W. McGowan, and S.A. Lee, *Phys. Rev. Lett.* **75**, 2638 (1995).
- [19] M. Kozuma, L. Deng, E.W. Hagley, J. Wen, R. Lutwak, K. Helmerson, S.L. Rolston, and W.D. Phillips, *Phys. Rev. Lett.* **82**, 871 (1999).
- [20] B. Paredes, A. Widera, V. Murg, O. Mandel, S. Fölling, I. Cirac, G.V. Shlyapnikov, T.W. Hänsch and I. Bloch, *Nature* **429**, 277 (2004).

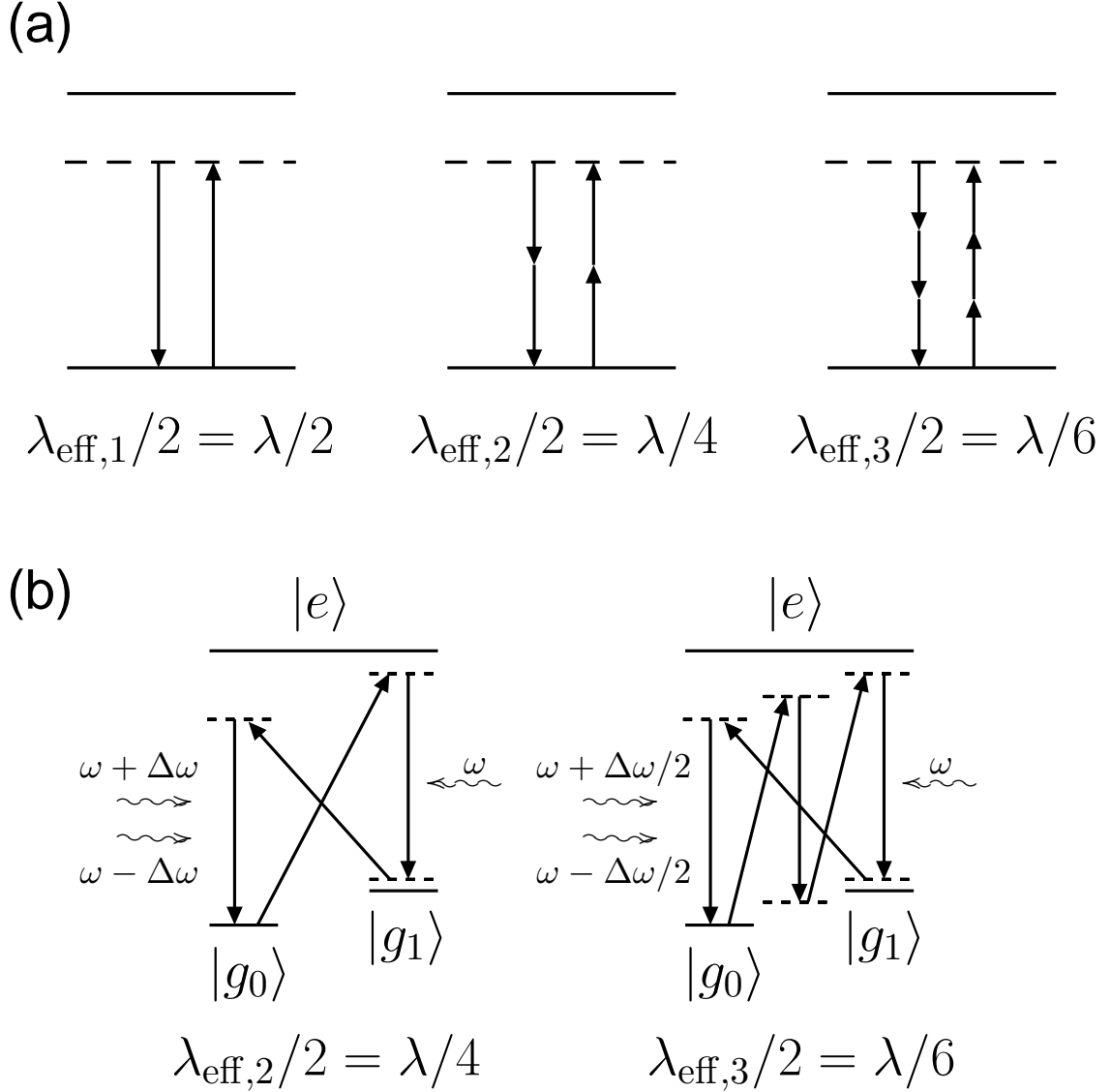


FIG. 1: Scheme for generation of lattice potentials with higher spatial periodicities. (a) Left: Second order processes in a usual standing wave lattice, yielding a spatial periodicity of $\lambda/2$ of the trapping potential. Middle and right: Four-photon (six-photon) processes contributing to a $\lambda/4$ ($\lambda/6$) spatial periodicity lattice potential. However, in these simple schemes the usual standing wave potential induced by two-photon processes dominates. (b) Improved scheme for generation of a four-photon (left) and six-photon (right) lattice potential, as used in this work. In contrast to the schemes indicated in (a), two-photon standing wave processes are here suppressed.

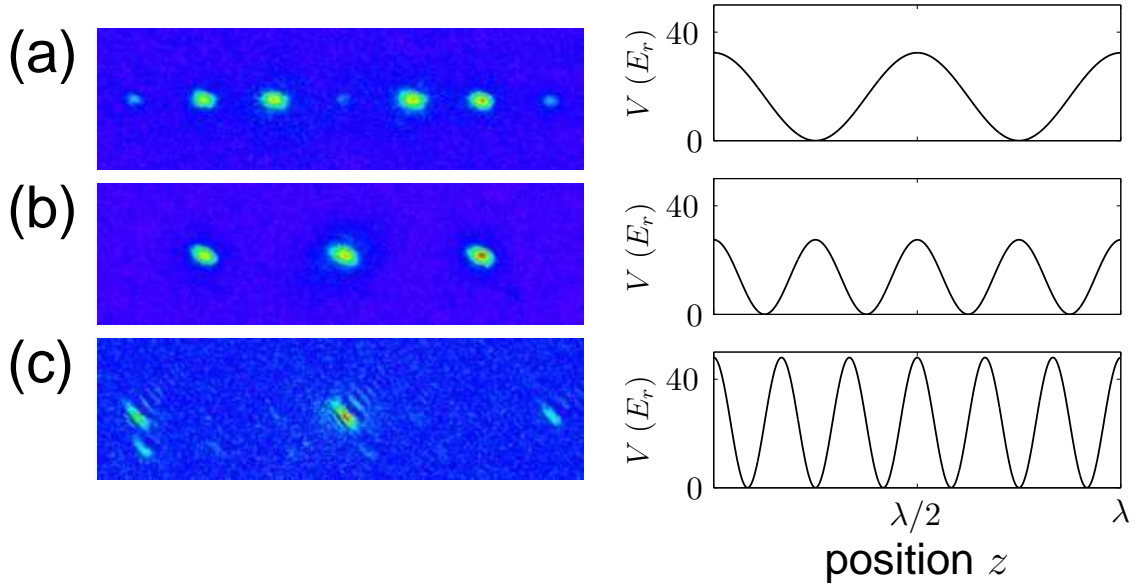


FIG. 2: The figures on the left hand side show the far-field diffraction images of a rubidium-Bose-Einstein condensate on (a) a usual standing wave lattice with $\lambda/2$ spatial periodicity, (b) a four-photon multiphoton lattice with $\lambda/4$ periodicity and (c) a six-photon lattice with $\lambda/6$ periodicity. A Stern-Gerlach magnetic field was applied in a angle of 45° relatively to the horizontal axis, which allows for a resolving of the atomic Zeeman structure. The figures on the right hand side show the corresponding reconstructed lattice potentials.

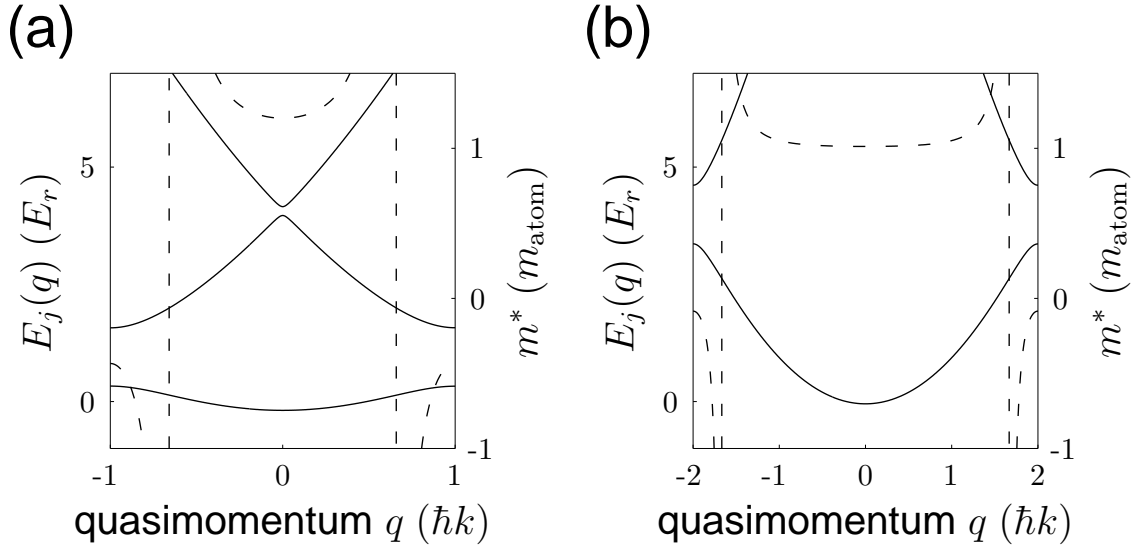


FIG. 3: Band structure (solid line) for atoms in a periodic lattice potential of (a) $\lambda/2$ and (b) $\lambda/4$ spatial periodicity respectively. The used lattice depth was $2.7 E_r$ in both cases. The dashed line shows the corresponding dependence of the effective atomic mass on the quasimomentum for an atom in the fundamental band.

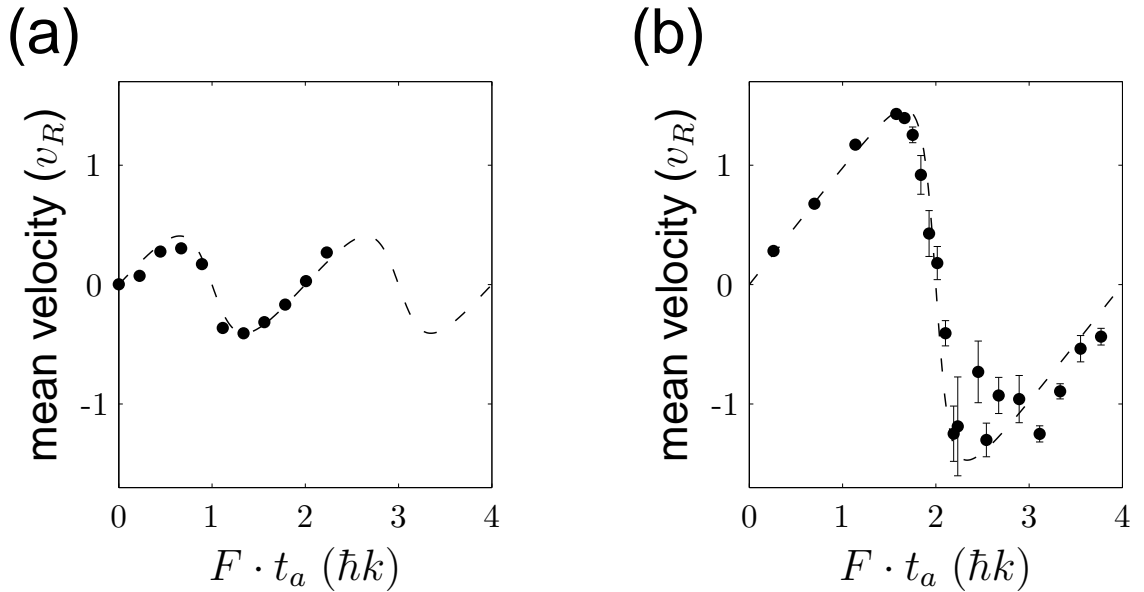


FIG. 4: Mean atomic velocity as a function of the acceleration time t_a for (a) a usual optical lattice and (b) a four-photon lattice with $\lambda/4$ spatial periodicity. For the data points with no visible error bar the corresponding uncertainty is below the drawing size of the dots.